Mg $3snf$-$3sng$-$3snh$-$3sni$ intervals and the Mg^+ dipole polarizability

B. J. Lyons and T. F. Gallagher
Department of Physics, University of Virginia, Charlottesville, Virginia 22901
(Received 31 October 1997)

We have observed the microwave transitions between the Mg $3snf$ states and the $3nsl$ states of $4 \leqslant l \leqslant 6$ using selective field ionization. The intervals can be analyzed using a core-polarization model in which the nonadiabatic effects are included with the quadrupole polarizability of the Mg^+ ion. Using this model we find the Mg^+ dipole polarizability $a_d = 33.80^{+0.50}_{-0.30} a_0^3$. We also find the nonadiabatic effects to cancel much of the effect of the quadrupole polarizability, a phenomenon also observed in He. [S1050-2947(98)01504-2]

PACS number(s): 32.30.Bv, 32.10.Dk

I. INTRODUCTION

In the alkaline-earth-metal atoms and He the bound Rydberg states are approximately equivalent since in both cases the Rydberg electron is outside a ''one-electron'' core, inviting comparisons between the two. The energies of He $1snl$ states of $l \geqslant 2$ are given to a good accuracy by a core-polarization model [1–3], and in the simplest form of this model the energy of a He $1snl$ state is expressed, in atomic units, as [1–3]

$$W_{nl} = -\frac{1}{2n^2} - \frac{\alpha_d}{2}\langle r^{-4}\rangle_{nl} - \frac{\alpha_q}{2}\langle r^{-6}\rangle_{nl}. \qquad (1)$$

Here α_d and α_q are the dipole and quadrupole polarizabilities of He^+, r is the distance from the He^+ to the Rydberg electron, and $\langle r^k\rangle_{nl}$ is the expectation value of r^k for the Rydberg electron in a hydrogenic nl orbit. Both components of the polarization potential lead to attractive forces on the Rydberg electron by the core, lowering the energy of the $1snl$ Rydberg state. There are several assumptions made in writing the energy as we have done in Eq. (1). First, we assume that the outer nl electron orbit does not penetrate the inner $1s$ electron orbit, and in the He $1sns$ and $1snp$ states the penetration precludes the use of the core-polarization model. Second, we assume that the outer electron is static, at least on the time scale of the motion of the inner electron. Finally, we assume the outer electron to be in a hydrogenic orbit.

Equation (1) gives an excellent representation of the energies of the He $1snl$ states for $l \geqslant 3$ [4]. For example, the $1snf$-$1sng$ and $1sng$-$1snh$ intervals calculated using Eq. (1) are within 5% and 2%, respectively, of the experimentally measured intervals [4,5]. In contrast, the d-f intervals calculated using Eq. (1) are more than 50% too high [6]. One of the sources of the discrepancy is that the second assumption made above is not completely correct; the outer electron is not static and its motion plays an important role, producing a repulsion between the electron and the ion. To account for the electron's motion a nonadiabatic correction must be introduced into Eq. (1) [7]. As pointed out by Callaway *et al.* [7], at long range this nonadiabatic correction scales as r^{-6} and we accordingly modify Eq. (1) to read

$$W_{nl} = -\frac{1}{2n^2} - \frac{\alpha_d}{2}\langle r^{-4}\rangle_{nl} - (\alpha_q - \beta)\langle r^{-6}\rangle_{nl}, \qquad (2)$$

where β, which is positive, represents the nonadiabatic correction. For He, α_d, α_q, and β are all calculable and Deutsch has shown that when the nonadiabatic correction is introduced the discrepancy between the calculated and observed He $1snd$-$1snf$ intervals is substantially reduced, to 20% [4]. Another interesting aspect of his calculations is that the nonadiabatic correction cancels the contribution of the quadrupole polarizability to within 5%.

The only alkaline-earth-metal atom in which measurements of intervals between several high-l series have been made is Ba [8]. However, the presence of low-lying states of Ba^+ makes Ba quite different from He, although some similarities remain. In contrast, in Mg^+ the excited states of the ion are all more than 35 000 cm^{-1} above the Mg^+ ground state, and it is reasonable to expect the bound Rydberg states of Mg to have energy levels that can be described in the same way as those of He. With this in mind we have measured the Mg $3snf$-$3sng$-$3snh$-$3sni$ intervals using a microwave resonance technique. In the section immediately following we describe our experimental approach and observations. We then describe how the Mg^+ dipole polarizability can be extracted from our data and compare our value with those obtained by others.

II. EXPERIMENTAL APPROACH

The essence of the experimental approach is easily understood with the aid of the level diagram of Fig. 1. Mg atoms are excited by three dye laser pulses via the sequence $3s^2 \rightarrow 3s3p \rightarrow 3snd \rightarrow 3snf$. Atoms in the $3snf$ states are then exposed to a 1-μs microwave pulse, which, on resonance, drives them to the $3snl$ ($l > 3$) state. Those atoms that have undergone the $3snf$-$3snl$ transition are detected by selective field ionization.

The Mg atoms effuse from a heated oven and are collimated to a beam 4 mm in diameter before passing midway between two aluminum plates 2.54 cm apart. The atoms are excited between the plates by the three overlapping laser beams propagating in the direction perpendicular to the atomic beam's propagation direction. The dye lasers are all of the Littman-Metcalf design [9] and are pumped by the second harmonic of a Nd:YAG laser (where YAG denotes

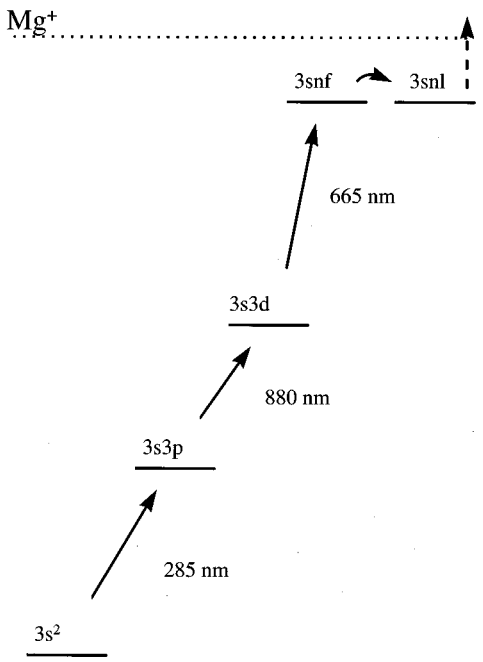

FIG. 1. Level diagram showing the three-step laser excitation by solid straight arrows, the microwave transition by a curved arrow, and field ionization by a broken arrow.

yttrium aluminum garnet) running at a 20-Hz repetition rate. The dye lasers have 1 cm^{-1} linewidths and 1 mJ pulse energies. The laser used to drive the Mg resonance line is frequency doubled in a potassium dihydrogen phosphate crystal, producing 50-μJ ultraviolet pulse energies.

Hewlett-Packard (HP) 8350B and 8290 sweep oscillators are used to generate microwaves from 8–26 GHz and a HP 5243 counter is used to measure the microwave frequency. The continuous-wave output of the sweep oscillators is passed through a variable attenuator and formed into pulses using a General Microwave FM862B switch, then amplified with a HP 8449B amplifier to powers of up to 100 mW. To generate frequencies from 26 to 40 GHz we pass (13 to 20)-

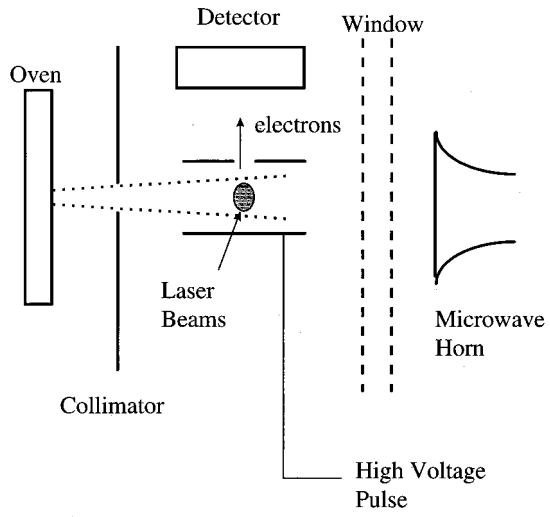

FIG. 2. Schematic diagram of the apparatus.

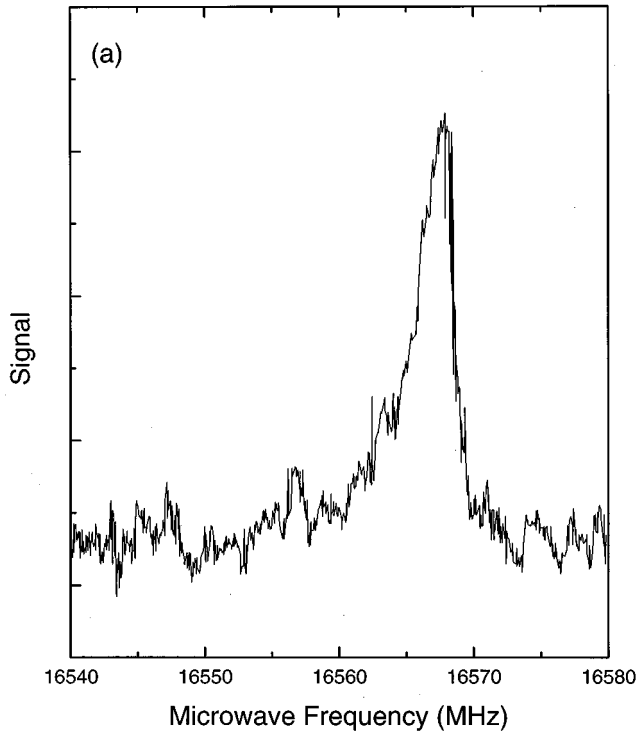

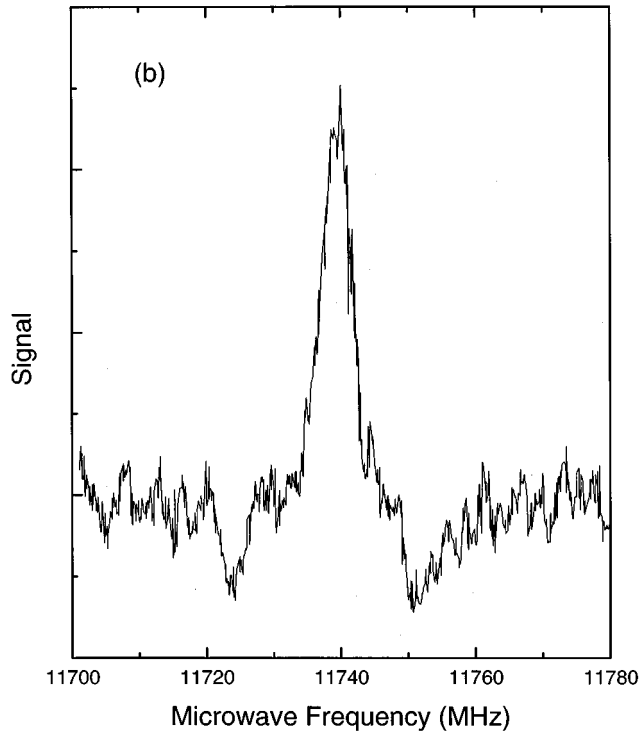

FIG. 3. Recordings of the (a) $3s21f$-$3s21h$ resonance and (b) $3s21f$-$3s21i$ resonance.

GHz pulses through a HP 83554A frequency doubler, generating ~5-mW pulses. In all cases the microwaves are brought to the interaction region by a waveguide. The microwaves propagate into the interaction region from a horn as shown in Fig. 2, and the waveguide and horn are outside the vacuum system, allowing the waveguide band to be changed without opening the vacuum chamber.

A negative high-voltage pulse is applied to the lower plate to ionize the Mg Rydberg atoms and drive the resulting elec-

TABLE I. Observed frequencies, with statistical uncertainties.

n	$3snf$-$3sng$ (MHz)	$3snf$-$3snh$ (MHz)	$3snf$-$3sni$ (MHz)
17		31 115(3)	
18		26 240(1)	
19	36 007(1)	22 340(1)	
	36 010(1)		
20	30 898(2)	17 168(1)	
21	26 707(2)	19 167(1)	11 739(2)
22		14 415(1)	10 212(2)
23		12 622(1)	

trons to a microchannel plate detector. The amplitude of the field pulse is set so as to ionize atoms in the $3snl$ ($l>3$) state, but not those in the $3snf$ state. The signal from the microchannel plates is captured with a gated integrator and stored in a computer as the microwave frequency is scanned through the resonance over many shots of the laser. Typical recordings of resonances are shown in Fig. 3 for the $3s21f$-$2s21h$ and $3s21f$-$3s21i$ two- and three-photon resonances.

We attempted to measure the shifts of the two-photon $3snf$-$3snh$ and three-photon $2snf$-$3snl$ resonances with microwave power, but were unable to detect the shifts. They are evidently less than the observed linewidths. To estimate the stray electric fields present we have measured the $3s21f$-$3s21g$ resonance as a function of applied static field. These measurements indicated vertical stray fields as large as 0.3 V/cm at the nominal zero field. We cannot directly measure the horizontal stray field, but see no reason for it to be as large as the vertical field. Consequently, 0.5 V/cm is a reasonable upper limit to the total stray electric field. The observed frequencies are given in Table I. The uncertainties are statistical and do not include any contribution from possible stray field shifts. The frequencies are equal to the $3snf$-$3sng$ intervals, half the $3snf$-$3snh$ intervals, and one-third of the $3snf$-$3sni$ intervals.

III. ANALYSIS

Using the $3snf$-$3snh$ and $3snf$-$3sni$ intervals implied by Table I, we have generated $3sng$-$3snh$ and $3snh$-$3sni$ intervals and fit them, together with the observed $3snf$-$3sng$ intervals, to the core-polarization model of Eq. (2). We have used the notation of Edlen [3], and, following the procedure of Safinya, Gallagher, and Sandner [10], we have recast Eq. (2) into the form

$$W_{nl}=-\mathcal{R}/n^2-\alpha_d P_{nl}-(\alpha_q-\beta)Q_{nl}, \tag{3}$$

where $\mathcal{R}$ is the Rydberg constant for Mg, 109 734.8 cm^{-1}, and W_{nl} is the energy of the Mg $3snl$ state in cm^{-1},

$$P_{nl}=\mathcal{R}\langle r^{-4}\rangle_{nl}, \quad Q_{nl}=\mathcal{R}\langle r^{-6}\rangle_{nl}.$$

The energy difference between the $3snl$ and $3snl'$ states is given by

$$\Delta W=W_{nl'}-W_{nl}=\alpha_d\Delta P+(\alpha_q-\beta)\Delta PQ, \tag{4}$$

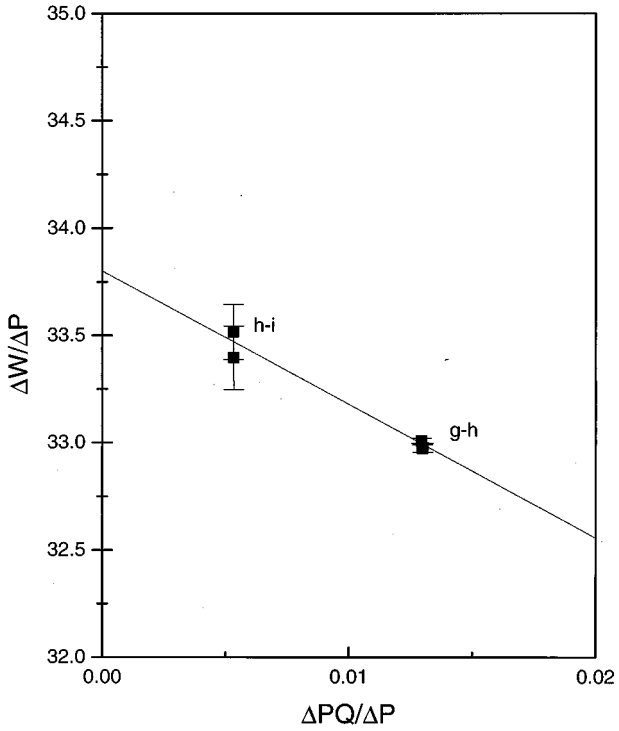

FIG. 4. Plot of the measured values of $\Delta W/\Delta P$ vs $\Delta PQ/\Delta P$ using the g-h and h-i intervals extracted from Table I.

where $\Delta P=P_{nl}-P_{nl'}$ and $\Delta PQ=P_{nl}Q_{nl}-P_{nl'}Q_{nl'}$. Dividing Eq. (4) by ΔP gives

$$\frac{\Delta W}{\Delta P}=\alpha_d+(\alpha_q-\beta)\frac{\Delta PQ}{\Delta P}. \tag{5}$$

On a graph of $\Delta W/\Delta P$ vs $\Delta PQ/\Delta P$, α_d is the vertical axis intercept and $\alpha_q-\beta$ the slope. Using the intervals derived from Table I, we have made such a graph, as shown in Fig. 4. Obviously, all the points do not fall on a line, and we must first decide which ones should. We presume that the Mg $3snf$ states exhibit core penetration, making the $3snf$-$3sng$ intervals larger than expected on the basis of core polarization alone. Support for this suggestion comes from comparing Mg to He. In He the $1snp$ states exhibit substantial core polarization, while in the $1snd$ states it is minimal. The classical outer turning point r_0 for a He^+ $1s$ electron is $r_o=1a_0$, while the inner classical turning points for He np and nd Rydberg electrons are $r_i=1a_0$ and $3a_0$. The ratios $R=r_i/r_o$ are 1 and 3, respectively, for the He $1snp$ and $1snd$ states. In the former substantial core penetration occurs, but in the latter it is effectively absent. In Mg^+ the outer turning point for the $3s$ electron is $3.63a_0$, while the inner turning points of the Mg nf and ng electrons are $6a_0$ and $10a_0$ respectively. Thus, for the Mg $3snf$ and $3sng$ states $R=1.65$ and 2.75 and, comparing He to Mg, we can reasonably expect the $3snf$ states to be penetrating, but not the $3sng$ states. Accordingly, we have fit only the $3sng$-$3snh$ and $3snh$-$3sni$ intervals to Eq. (5), resulting in the solid line shown in Fig. 4.

As mentioned above, we cannot exclude the possibility of stray electric fields and their effect is most pronounced on

TABLE II. Mg^+ dipole polarizabilities.

Experimental (α_0^3)	Theoretical (α_0^3)
34.62(26)[a]	34.144[a]
33.0(5)[b]	33.9[c]
	37.22[d]
	38.94[e]
	34.05[f]
	38.7[g]

[a]See Ref. [15].
[b]See Ref. [14].
[c]See Ref. [17].
[d]See Ref. [11].
[e]See Ref. [18].
[f]See Ref. [12].
[g]See Ref. [13].

the $3sni$ states. We calculate that a stray field of 0.5 V/cm would depress the energies of the $3s21i$ and $3s22i$ states by 20 and 28 MHz, respectively. Thus the measured intervals are lower limits to the actual intervals. We have accordingly raised the upper uncertainty limits on the n-i points of Fig. 4 to reflect the possible Stark shifts, resulting in $\alpha_d = 33.80^{+0.50}_{-0.30} a_0^3$ and $\alpha_q - \beta = -62.2^{+20}_{-15} a_0^5$.

Although we have no way to separate α_q from β using our experimental data, we can use the theoretical values for α_q to estimate the nonadiabatic parameter β. There are three theoretical values for α_q, ranging from $150a_0^5$ to $187a_0^5$ [11–13]. Accordingly, $200a_0^5 < \beta < 250a_0^5$. In other words, α_q and β are roughly the same size, although not so close as in He.

It is useful to compare our value of α_d with those obtained by others, and in Table II we list the other values. Two are derived from experimental data. From optical $3sng$-$3sn'h$ and $3snh$-$3sn'i$ transitions Chang and Noyes [14] extracted the value $\alpha_d = 33.6a_0^3$. They ignored the quadrupole polarizability, which works well since $\alpha_q \approx \beta$. Theodosiou *et al.* [15] used the measured Mg^+ $3p_j$ lifetimes [16] to obtain values for the Mg^+ $3s_{1/2}$-$3p_j$ oscillator strengths, which are responsible for 99% of α_d, and calculated the oscillator strengths to higher-lying Mg^+ np states. From these oscillator strengths they determined $\alpha_d = 34.62(26)a_0^3$, a value that clearly differs from ours, although the error bars overlap. As shown by Table II, the purely theoretical values [12–14,16–18] cover a rather broad range, bracketing the experimental numbers.

IV. CONCLUSION

We have measured the Mg $3snf$-$3sng$-$3snh$-$3sni$ intervals using a microwave resonance technique and extracted from these intervals a value for the Mg^+ dipole polarizability. We have used a core-polarization model, in which the leading nonadiabatic correction appears in the same way as does the quadrupole polarizability, to determine α_d and the difference in the two parameters α_q and β. While we cannot determine α_q and β individually, we find that they are of approximately the same size, largely offsetting each other, but not quite to the extent as occurs in He. Our value of the dipole polarizability α_d is slightly lower than the presumably most reliable determination, based on Mg^+ lifetime experiments. It seems quite possible that the discrepancy might arise from a shortcoming of the model we have used to analyze our data. For this reason and to assess the relative importance of penetration and nonadiabatic effects in the $3snf$ states it would be used to have more accurate calculations of the Mg atomic structure.

ACKNOWLEDGMENT

This work was supported by the U.S. Department of Energy, Office of Basic Energy Sciences.

[1] I. Waller, Z. Phys. **38**, 689 (1926).
[2] J. E. Mayer and M. G. Mayer, Phys. Rev. **43**, 605 (1933).
[3] B. Edlen, in *Atomic Spectra*, edited by S. Flugge, Handbuch der Physik Vol. XXVII (Springer-Verlag, Berlin, 1964).
[4] C. Deutsch, Phys. Rev. A **2**, 43 (1970).
[5] D. R. Cok and S. R. Lundeen, Phys. Rev. A **23**, 2488 (1981).
[6] J. W. Farley, K. B. MacAdam, and W. H. Wing, Phys. Rev. A **20**, 1754 (1979).
[7] J. Callaway, R. W. Labahn, R. T. Pu, and W. M. Duxler, Phys. Rev. **168**, 12 (1968).
[8] T. F. Gallagher, R. Kachru, and N. H. Tran, Phys. Rev. A **26**, 2611 (1982).
[9] M. G. Littman and J. H. Metcalf, Appl. Opt. **17**, 2224 (1978).
[10] K. A. Safinya, T. F. Gallagher, and W. Sandner, Phys. Rev. A **22**, 2672 (1981).
[11] P. W. Langhoff and R. P. Hurst, Phys. Rev. **139**, A1415 (1965).
[12] S. A. Adelman and A. Szabo, J. Chem. Phys. **58**, 687 (1973).
[13] S. J. Easa and G. C. Shukla, J. Phys. (Paris) **40**, 137 (1989).
[14] E. S. Chang and R. W. Noyes, Astrophys. J. **275**, L11 (1983).
[15] C. E. Theodosiou, L. J. Curtis, and C. A. Nicolaides, Phys. Rev. A **52**, 3677 (1995).
[16] W. Ansbacher, Y. Li, and E. H. Pinnington, Phys. Lett. A **139**, 165 (1989).
[17] L. J. Curtis, Phys. Scr. **21**, 162 (1980).
[18] B. Kundu, D. Ray, and P. K. Muckerjee, Phys. Rev. A **34**, 62 (1986).